

# Snow-fed streamflow timing at different basin scales: Case study of the Tuolumne River above Hetch Hetchy, Yosemite, California

Jessica D. Lundquist<sup>1</sup>

Scripps Institution of Oceanography, La Jolla, California, USA

Michael D. Dettinger<sup>2</sup>

U.S. Geological Survey, La Jolla, California, USA

Daniel R. Cayan<sup>3</sup>

Scripps Institution of Oceanography, La Jolla, California, USA

Received 29 December 2004; revised 22 March 2005; accepted 29 March 2005; published 7 July 2005.

[1] Diurnal cycles in snow-fed streams provide a useful technique for measuring the time it takes water to travel from the top of the snowpack, where snowmelt typically peaks in the afternoon, to the river gauge, where the daily maximum flows may arrive many hours later. Hourly stage measurements in nested subbasins (6–775 km<sup>2</sup>) of the Tuolumne River in Yosemite National Park illustrate travel time delays at different basin scales during the spring 2002 and 2003 melt seasons. Travel times increase with longer percolation times through deeper snowpacks, increase with longer travel times over land and along longer stream channels, and increase with slower in-stream flow velocities. In basins smaller than 30 km<sup>2</sup>, travel times through the snowpack dominate streamflow timing. In particular, daily peak flows shift to earlier in the day as snowpacks thin and mean discharges increase. In basins larger than 200 km<sup>2</sup>, snowpack heterogeneity causes the hour of peak flow to be highly consistent, with little or no variation as the snowpack thins. Basins with areas in between 30 and 200 km<sup>2</sup> exhibit different sequences of diurnal streamflow timing in different years, sometimes acting like small basins and other times like large basins. From the start of the melt season until the day of peak snowmelt discharge, increasing travel distances in channels as the snow line retreats to higher elevations do not cause long enough travel delays to offset the observed decrease in mean travel times through the snowpack. A model that couples porous medium flow through thinning snowpacks with free surface flow in stream channels can reproduce the observed patterns, provided that the model incorporates snowpack heterogeneity.

**Citation:** Lundquist, J. D., M. D. Dettinger, and D. R. Cayan (2005), Snow-fed streamflow timing at different basin scales: Case study of the Tuolumne River above Hetch Hetchy, Yosemite, California, *Water Resour. Res.*, 41, W07005, doi:10.1029/2004WR003933.

## 1. Introduction

[2] Diurnal fluctuations, generally observed in hourly streamflow measurements from snow-fed watersheds, provide a new way of understanding basin hydrology. The daily cycle of solar forcing yields major changes in snowmelt and streamflow over the course of each day, and the difference between the time of highest melt rate and the time of peak runoff provides a measure of average runoff travel times through the river basin (Figure 1). These travel times provide information about snowpack properties, in-channel

flow velocities, and distances to the primary snowmelt source areas. The ability to predict travel times may prove useful for flood forecasting, reservoir and hydropower operations, and characterizing and predicting chemical transports in mountain rivers.

### 1.1. Prior Studies

[3] Most previous studies of short-term streamflow timing variations have focused on small basins and local processes [Bengtsson, 1981; Caine, 1992; Colbeck, 1972; Dunne et al., 1976; Jordan, 1983; Woo and Slaymaker, 1975]. Braun and Slaymaker [1981] examined changes in diurnal runoff at different spatial scales, but their largest basin, Miller Creek, encompassed only 23 km<sup>2</sup>. Kobayashi and Motoyama [1985] examined streamflow timing in four adjacent watersheds from 0.4 to 108 km<sup>2</sup>, all completely snow covered throughout the period of study. All of these studies report that travel times decrease as the snowpack

<sup>1</sup>Now at Climate Diagnostics Center, Cooperative Institute for Research in Environmental Sciences, Boulder, Colorado, USA.

<sup>2</sup>Also at Scripps Institution of Oceanography, La Jolla, California, USA.

<sup>3</sup>Also at U.S. Geological Survey, La Jolla, California, USA.

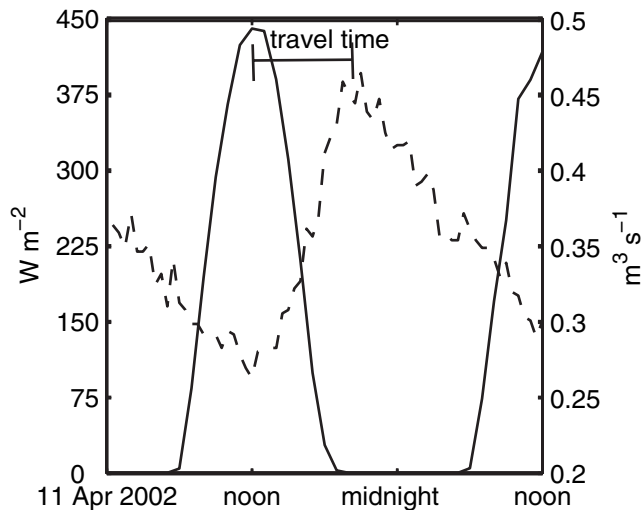


**Figure 1.** Travel time, which can be measured as the difference between the time of peak solar radiation (solid line) and the time of peak discharge (dashed line).

thins and matures, reflecting shorter travel times for meltwater to pass from the snow surface to the base of the snowpack.

[4] Basin-scale runoff travel times cease to be dominated by snowpack properties when larger basins are considered. *Grover and Harrington* [1966] state that below the snowfield, peaks and troughs of the diurnal cycle occur later than at the edge of a snowfield, with a delay that depends on the in-stream distance from the snowfield and on the stream's velocity. *Lundquist and Cayan* [2002] show that, during the peak melt season, most USGS gauged rivers in the western United States have clear diurnal cycles, and that the hour of peak flow changes very little during the peak melt season. The mechanisms by which the evolution of diurnal cycles in many small ( $<30 \text{ km}^2$ ) catchments or subcatchments sum to form the contrasting evolution of diurnal cycles in larger ( $>200 \text{ km}^2$ ) basins, however, has not been described previously.

## 1.2. Current Study: Tuolumne River, Yosemite National Park

[5] This paper presents an analysis of new observations of hourly streamflow timing within nested basins of the Tuolumne River above the Hetch Hetchy Reservoir, Yosemite National Park, California (Figure 2). California has a Mediterranean climate, and most precipitation falls between November and March. Thus snow provides a natural reservoir, releasing winter precipitation in the summer when the population needs it most. Indeed, over half of California's water supply comes from the high-elevation snowpacks of the Sierra Nevada. Climate variability in the region is high, and precipitation and runoff fluctuate from year to year, from under 50% to over 200% of climatological averages. Climate fluctuations, climate trends, and the growing needs of water consumers require informed management of these resources. In order to improve understanding of hydrologic processes at high altitudes, a network of meteorological and hydrological sensors has been deployed in Yosemite National Park since Summer 2001 [*Lundquist et al.*, 2003].

[6] The nested subbasins in the study area illustrate the kinematics of streamflow timing at different spatial scales. During the 2002 and 2003 melt seasons, in-stream pressure sensors (Solinst Leveloggers, <http://www.solinst.com>) measured river stages at half-hour intervals in 17 subbasins (Figure 2) of the Tuolumne and Merced rivers. Subbasin areas, delineated on a 30-m resolution digital elevation model (DEM), range from 6 to  $775 \text{ km}^2$ . Basin elevations range from 1200 to 3700 m. Table 1 details the characteristics of three subbasins examined in this paper.

[7] During the first half of the 2002 and 2003 melt seasons, from the day flows started rising until the day of peak flow, different sized basins exhibited different trends in diurnal streamflow timing (Figure 3). During this early season melt period, sensors monitoring flows from basins larger than  $200 \text{ km}^2$  reported remarkably constant diurnal streamflow timings, e.g., at Glen Aulin ( $251 \text{ km}^2$ ) and Hetch Hetchy ( $775 \text{ km}^2$ , Figure 3). This consistency is similar to that observed in most USGS gauged basins throughout the western United States [*Lundquist and Cayan*, 2002; *Lundquist*, 2004; *Lundquist and Dettinger*, 2005].

[8] In the subbasins smaller than  $30 \text{ km}^2$ , e.g., in Rafferty Creek ( $25 \text{ km}^2$ , Figure 3), the observed times of peak daily flows evolved so that they were 5 to 6 hours earlier on the day of peak flow than they were when flows began to rise in both years. This evolution is similar to the sequence of events reported by previous small basin studies [*Bengtsson*, 1981; *Caine*, 1992; *Colbeck*, 1972; *Dunne et al.*, 1976; *Jordan*, 1983]. At gauges monitoring subbasins larger than  $30$  but smaller than  $200 \text{ km}^2$ , the evolution of daily flow timing differed from one spring to the next. In 2002, at the Lyell Fork of the Tuolumne River ( $109 \text{ km}^2$ , Figure 3), daily peak flows arrived between 2000 and 2200 local standard time (LST) during the early melt season, with no clear trend toward earlier or later diurnal cycles, a seasonal evolution similar to those in the larger basins. In 2003, however, streamflow timing at Lyell Fork came earlier as the melt season progressed, until by the day of peak flows, the diurnal peak was 3 hours earlier than when the snowmelt began. Thus flows in 2002 evolved like a large basin, and flows in 2003 evolved more like a small basin.

[9] Following the day of peak spring discharge, during the second half of the two melt seasons, the peak daily flows arrived later and later in all basins, even as flows declined. During this period of declining streamflow, more and more of the snowmelt originated from the highest snowfields, and streamflow velocities decreased as water levels in the channels fell [*Rickenmann*, 1994]. The resulting delays in diurnal cycle timing were greatest in the larger basins, where long travel distances added significantly to time delays caused by declining velocities. This period of declining streamflow is the subject of continuing research and is not the focus of this paper.

## 1.3. Objectives

[10] This study focuses on the basin-to-basin and, in some basins, year-to-year differences in diurnal streamflow timing during the period in early spring from the start of snowmelt to the date of peak discharge. Somehow, discharge from numerous small ( $<30 \text{ km}^2$ ) catchments, each with diurnal peak streamflows that arrive earlier each day as the snowpack shrinks, combine to produce a diurnal signal

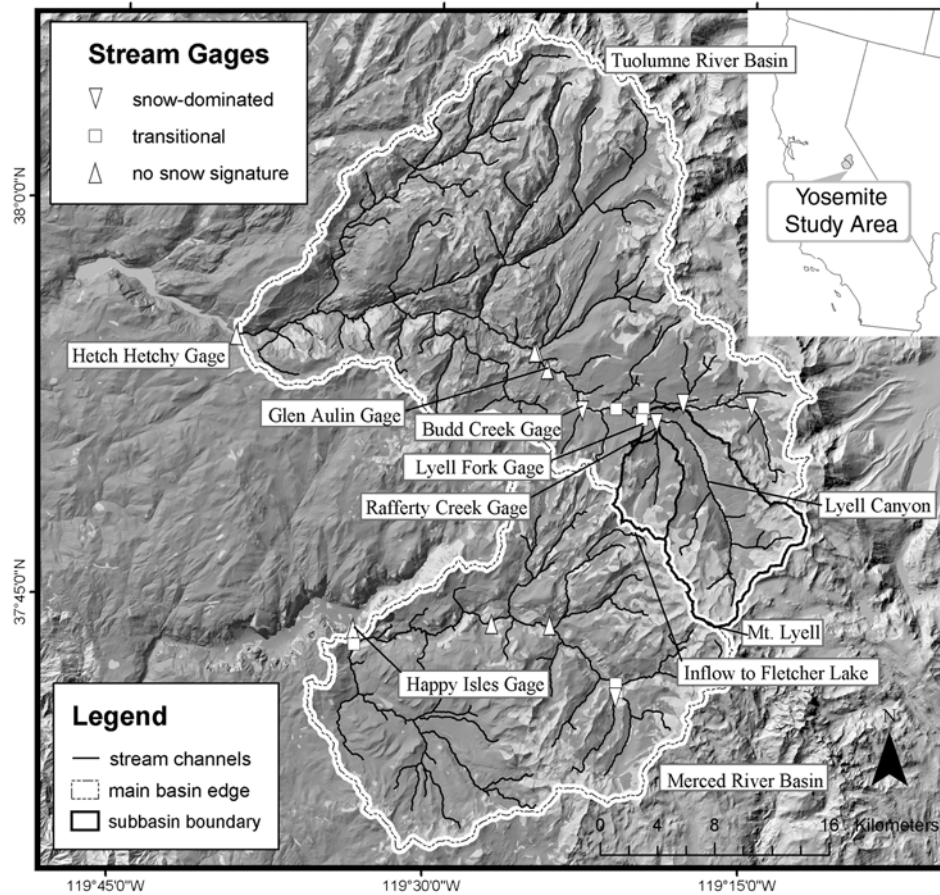


**Figure 2.** Map of stream gauges in intensive study area in Yosemite National Park. Gauges marked as “snow-dominated” monitor basins with areas less than 30 km<sup>2</sup>. Gauges marked as “transitional” monitor basins larger than 30 km<sup>2</sup> but smaller than 200 km<sup>2</sup>. Gauges marked as “no snow signature” monitor basins larger than 200 km<sup>2</sup>.

in larger (>200 km<sup>2</sup>) catchments that peaks near the same time each day during this period, apparently regardless of snowpack properties. This change could come about because the time that water spends moving through the snowpack becomes a smaller fraction of the total travel time as channel distances and channel travel times increase with basin scale. The change could occur because small headwater basins are snow covered throughout the first half of the melt season, whereas larger basins generally span larger ranges of elevations and have snow lines that retreat to higher altitudes during the melt season. In these larger basins, the increase in travel distance along the channels might offset the decrease in travel distance through the snowpack. However, this possibility would require some unrealistic “tuning” of the rates of snow line retreat to just match the hastening of diurnal cycles expected from snowpack thinning.

[11] Alternatively, variations in snow depths and melt rates are observed to increase with basin scale [Anderton *et al.*, 2002; Erxleben *et al.*, 2002]. These spatial variations of snowpack properties within the larger basins would yield differing contributions to the diurnal cycles of streamflow, contributions that peak at very different times of day. The timing of the sum of all these contributions ends up being independent of the snowpack properties at any one point [Lundquist and Dettinger, 2005; Lundquist, 2004]. The resulting diurnal timing is stable throughout the early melt season because of the (essentially random) heterogeneity of the snowpack rather than because of a specific spatial distribution of snowpack properties.

[12] The present analysis uses the Tuolumne River network of streamflow observations along with a numerical simulation to test the above hypotheses. The average time that meltwater spends in the snowpack on various days

**Table 1.** Tuolumne River Subbasin Characteristics

Basin	Area, km <sup>2</sup>	Main Channel Length, km	Gauge Elevation, m	Mean Elevation, m	Highest Elevation, m
Rafferty Creek	25	9	2670	3060	3400
Lyell Fork	109	20	2670	3160	3700
Hetch Hetchy	775	59	1170	2850	3700

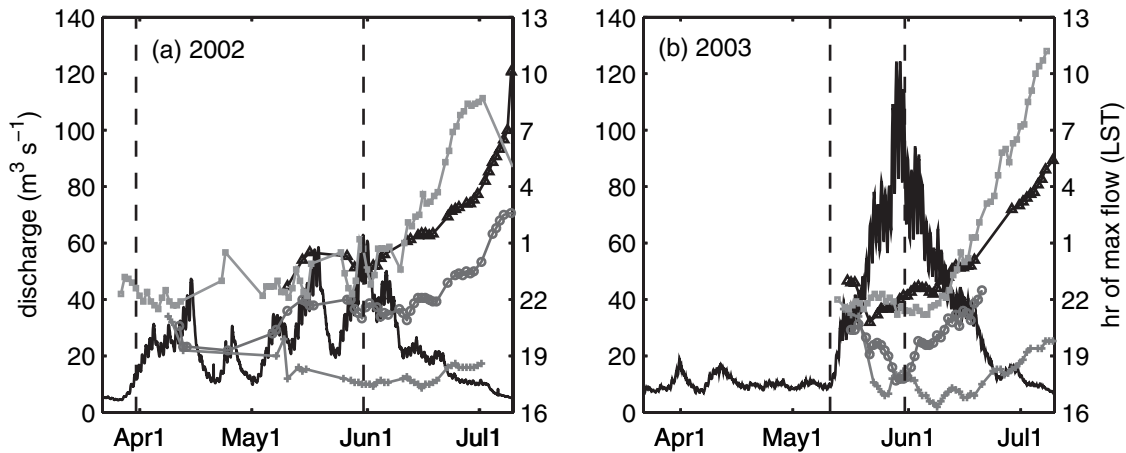


**Figure 3.** Observations of hour of peak streamflow (curves with symbols, right axis) in local standard time (LST) for Rafferty Creek (pluses), Lyell Fork (circles), Glen Aulin (triangles), and Hetch Hetchy (squares) along the Tuolumne River in (a) 2002 and (b) 2003. Discharge at the nearby Merced River at Happy Isles gauge (solid line, left axis), which is highly correlated with stages at all gauges, illustrates relative discharge magnitudes through time. Vertical dashed lines indicate the beginning and end of the period of interest for this study. The falling limb of the hydrograph is not considered here.

during the early melt season is estimated from measurements of snow depth and melt rates (section 2.1). The average time spent traveling along the stream channel is estimated using observed distances along channels from the snow line to a gauge together with estimates of in-channel velocities for a measured discharge (section 2.3). These estimates, although approximate, indicate that the travel times in stream channels are short compared to travel times within the snowpack, even in the large Hetch Hetchy basin (775 km<sup>2</sup>). Increases in channel lengths from retreating snow lines to the gauges are not sufficient to offset the decreasing travel times through the thinning snowpack (section 2.4). Thus some other property that changes with basin scale must be responsible for the observations of streamflow timing. Variability in snowpack properties increases in larger basins, and a simulation of the Tuolumne River above Hetch Hetchy is used to test how snowpack variability affects streamflow timing at different scales (section 3). As with the travel time estimates of section 2, the model shows that the seasonal evolution of in-channel travel velocities and distances is not sufficient to explain the observed timing changes. Rather, the model must include heterogeneity of snowpack properties if it is to reproduce the observed patterns in streamflow timing. Thus accurate representations of snowpack heterogeneity appear to be essential for accurate forecasts of short-term streamflow timing (Section 4). Thus the heterogeneity of snow-fed river basins is an essential characteristic that affects their hydrologic behavior and not a source of “noise.”

## 2. Estimated Travel Times: Snowpack Versus Stream

[13] Average travel times in a basin are the average distances traveled divided by the path-averaged travel velocities, along flow paths from melt to measurement. The path-averaged distances depend on (1) distances that meltwater has to percolate through the snowpack, (2) paths and distances traveled from the base of the snowpack to

channels, and (3) distances that the water flows along the channel network to reach the gauge. Travel velocities depend on discharge magnitude, geometry, and friction along these paths. As the snowmelt season begins, snowpacks mature, flow fingers develop, and stream channels fill so that flow velocities increase. Thus overall travel velocities increase in both snowpacks and river channels along with the increases in discharge. To interpret the observed sequences of daily flow times discussed in section 1, we partitioned travel times between travel in the snowpack and travel along the hillslope and stream channel. Adding a snowpack component to *D’Odorico and Rigon’s* [2003] estimated mean travel time across hillslopes and channels,  $E[t]$ , yields

$$E[t] = \frac{\langle x_s \rangle}{u_s} + \frac{\langle x_h \rangle}{u_h} + \frac{\langle x_c \rangle}{u_c} \quad (1)$$

where  $\langle x_{s/h/c} \rangle$  is the average travel distance and  $u_{s/h/c}$  is the average velocity of water through or over the snowpack<sub>(s)</sub>/hillslope<sub>(h)</sub>/channel<sub>(c)</sub>.

### 2.1. Travel Time Through the Snowpack

[14] To estimate travel times through the snowpack, one must know the distances water moves through the snowpack (snow depths) and the speed at which meltwater travels, which depends on surface melt rates and on snowpack properties. To estimate these time-varying properties, measurements of daily snow water equivalent (SWE) during springs 2002 and 2003 were analyzed at 47 snow pillows at elevations from 1500 to 3400 m throughout the central Sierra Nevada (described further by *Lundquist et al.* [2004]). Daily melt rates were estimated from the day-to-day differences in SWE at each station. This interpretation assumes that all of the meltwater migrated out of the snowpack above the pillow each day. While it accurately measures outflow from the snowpack and inflow to the stream, actual surface melt rates may be underestimated, particularly early in the season when melt at the upper surface is retained within the snowpack.

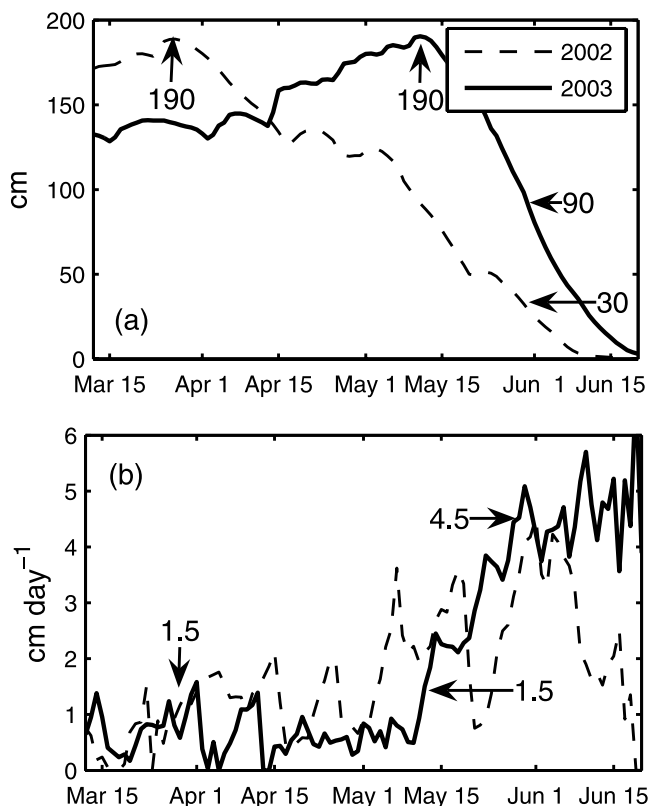


**Figure 4.** (a) Average snow depth versus day of the year for 2002 and 2003. Arrows indicate average depth at the start of the main melt season (time of peak snow accumulation) and on the day of peak discharge (30 May). (b) Average daily melt versus time for the 2 years. Arrows indicate melt rates at the start and peak of each melt season.

[15] Snow depth, density, and SWE were measured at 92 snow courses in the central Sierra Nevada on 1 April 2002 and 1 May 2003, near the start of the melt season for each year. The average density at these snow courses, calculated by combining both sets measurements, was  $400 \text{ kg m}^{-3}$ . Because density varies much less in space and time than either SWE or snow depth [Adams, 1976; Anderton *et al.*, 2002; Elder *et al.*, 1991; Logan, 1973; Shook and Gray, 1997], this average density was used to convert SWEs at the snow pillows to snow depths (Figure 4a). Density was assumed constant throughout the melt season, since sensitivity tests by Lundquist and Dettinger [2005] indicated that seasonal changes in density did not noticeably affect diurnal melt timing.

[16] Flow through snowpacks can be modeled as a vertical percolation of water through an unsaturated porous medium [Colbeck, 1972]. Although downslope flow along ice layers is likely throughout the Sierra Nevada [Kattelmann and Dozier, 1999], flow from the top to the bottom of the snowpack probably dominates the melt regime, especially on slopes of lower angle and when the snowpack is isothermal at  $0^\circ\text{C}$  [Smith, 1974; Dettinger and Gerke, 2002]. From a snowmelt propagation model [Dunne *et al.*, 1976], we estimate

$$u_s = Km^{2/3} \quad (2)$$

where  $u_s$  is the vertical velocity through the snowpack,  $m$  is the melt rate at the surface, and  $K$  corresponds to an unsaturated permeability, assumed herein to be about  $99 \text{ cm}^{1/3} \text{ h}^{-1/3}$  ( $1.4 \text{ m}^{1/3} \text{ s}^{-1/3}$ ), based on estimates by Lundquist and Dettinger [2005] and Lundquist [2004].

[17] On the basis of snow pillow measurements from 2002 and 2003 (Figure 4b), typical daily totals of snowmelt in the central Sierra range from  $1.5 \text{ cm d}^{-1}$ , early in the season, to  $4.5 \text{ cm d}^{-1}$ , during peak melt. On the basis of energy balance measurements and calculations from the Mammoth Mountain Energy Balance Monitoring Site (<http://neige.bren.ucsb.edu/mmsa/>), located southeast of the Yosemite Study area in the Sierra Nevada, melt rates follow the diurnal cycle of solar radiation. Thus melt rates can be represented by half sinusoids with peaks at noon each day. In this idealized representation, average daytime melt rates are assumed to vary from  $0.125$  to  $0.375 \text{ cm h}^{-1}$ , and maximum melt rates vary from  $0.196$  to  $0.589 \text{ cm h}^{-1}$ . Substituting these melt rates into equation 2, typical velocities range from  $25$  to  $70 \text{ cm h}^{-1}$ , consistent with values measured in previous field experiments:  $25 \text{ cm h}^{-1}$  [Dunne *et al.*, 1976],  $36 \text{ cm h}^{-1}$  [Colbeck and Anderson, 1982], and  $50 \text{ cm h}^{-1}$  [Kobayashi and Motoyama, 1985].

[18] Thus, given observations (or estimates) of snowpack thicknesses, travel time through snowpacks can be estimated throughout the melt seasons. At the start of the melt season in both 2002 and 2003, the snow depths at the snow pillows,  $\langle x_s \rangle$ , averaged  $190 \text{ cm}$ . Assuming  $m \cong 0.125 \text{ cm h}^{-1}$  and  $u_s = 25 \text{ cm h}^{-1}$ , the travel time through the snowpacks might have totaled as much as  $7.7$  hours. The snowmelt season was much shorter in 2003 than in 2002, due to above-normal April snowfall and therefore a late start of melt, but in both years peak flows occurred around 30 May, when average melt totals reached  $4.5 \text{ cm d}^{-1}$  (Figure 4b) and  $u_s = 50 \text{ cm h}^{-1}$ . By that time,  $\langle x_s \rangle = 30 \text{ cm}$  in 2002 and  $90 \text{ cm}$  in 2003. Consequently, by the end of May, snowpack travel times were about  $0.6$  hour and  $1.7$  hours in 2002 and 2003, respectively. Thus, from the beginning to midpoint of the 2002 and 2003 snowmelt seasons, the travel times through the snowpacks would be expected to have declined by  $6$  to  $7$  hours. This estimated reduction in travel time is consistent with observations in subbasins with areas less than  $30 \text{ km}^2$ , e.g., Rafferty Creek (Figure 3), in both years. Because the channel lengths are short in the smaller basins, the close agreement between this travel time estimate and observations suggests that meltwater percolates through the unsaturated snowpack at a speed that is consistent with equation 2.

## 2.2. Travel Time From the Snowpack to the Stream Channel

[19] Hillslope lengths,  $\langle x_h \rangle$ , have been parameterized by  $\frac{1}{2D}$  [Bras, 1990], where  $D$  is the watershed's drainage density, i.e., the total length of channels within a basin divided by the basin area. For the Tuolumne River drainage,  $D$  was estimated from a DEM (Figure 2), and  $\langle x_h \rangle \cong 250 \text{ m}$ . Estimates of  $u_h$  range from  $14 \text{ m h}^{-1}$  for travel along the saturated base of a snowpack [Dunne *et al.*, 1976] to  $540 \text{ m h}^{-1}$  for fast overland flow [Dunne, 1978]. Thus, in the Tuolumne River drainage, the time spent in hillslope transport could vary from less than one hour to just under a day. Neither drainage densities nor overland flow velocities depend much on basin size [D'Odorico and Rigon, 2003].

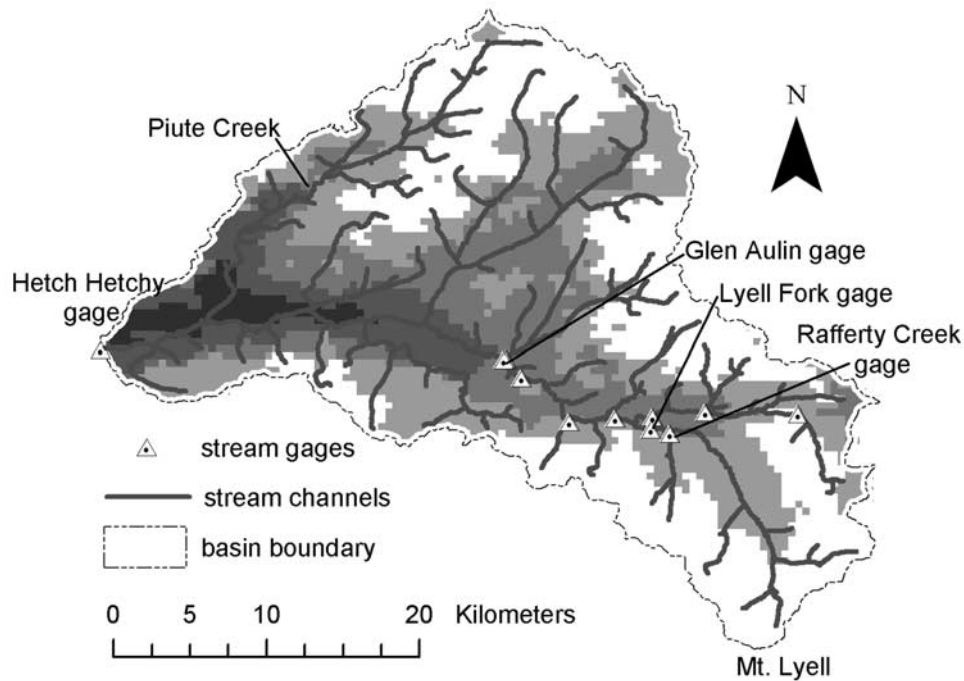


**Figure 5.** Map of snow cover for the Tuolumne River basin above Hetch Hetchy. Darkest to lightest shading represents area that was snow free from 9 May 2003 on, from 17 May, from 25 May, and by 2 June, respectively. White areas were snow covered on 2 June. The elevation ranges from 1200 m at the Hetch Hetchy gauge on the west side of the map to 3700 m at Mount Lyell on the southeast corner of the map.

Seasonal changes in soil moisture, frozen ground, and relative proportions of surface to subsurface flow are likely to affect diurnal timing at a site [Lundquist and Dettinger, 2005]. However, soil characteristics in the Tuolumne Watershed do not change systematically with basin scale. For example, most of the fine-grained soils are located in the Tuolumne Meadows region upstream of the Lyell Fork gauge, while most of the riverbed and adjacent slopes between the Glen Aulin and Hetch Hetchy gauges are bare granite. Thus, while time spent in hillslope transport might vary by up to 22 hours at different basin locations, these variations do not appear to depend on basin scale and thus probably are not responsible for the observed scale-dependent variations in timing. However, variability in hillslope transport is probably partly responsible for smoothing out the peak in the streamflow hydrograph. In this study, we assume hillslope transport is fast and neglect its influence on streamflow timing.

### 2.3. Travel Time Along the Stream Channel

[20] Estimating travel times in stream channels requires knowledge of channel lengths and path-integrated velocities. To determine how the distances from the snow line to each gauge increase as the snow line retreats to higher elevations, MODIS-derived snow covered area maps were obtained for the 2002 and 2003 melt seasons (MOD10A2 data product (Hall *et al.* [2000], data from March to June 2002 and May to June 2003)). These images had 500-m spatial and 8-day temporal resolution and were projected over the DEM (Figure 5). The changing snow line primarily follows contours of elevation. If most discharge had originated from the edge of the snow line along the

main channel of the Tuolumne River above Hetch Hetchy,  $\langle x_c \rangle = 16$  km on 09 May 2003, when melt began, and  $\langle x_c \rangle = 46$  km on 02 June 2003, when peak flow occurred. If all snow covered areas contributed equally to Tuolumne River discharge, then, by averaging over all the snow covered lengths of the channel network,  $\langle x_c \rangle = 33$  km on 09 May 2003, and  $\langle x_c \rangle = 40$  km on 02 June 2003. On 02 June, the area-averaged channel length is shorter than the main channel length because Piute Creek, in the northern portion of the basin, contributed snowmelt from a shorter distance than the main channel, which had a snow line near Mount Lyell (Figure 5).

[21] In-channel flow velocities depend strongly on channel geometry and roughness, which are difficult to parameterize [Bathurst, 2002]. Velocity increases with discharge [Rickenmann, 1994] and slope [Bras, 1990], but the coefficients and forms of the equations vary between river reaches. In-channel velocities can be estimated by the Manning and Chezy equations:

$$u_c = C(Q)\sqrt{s} \quad (3)$$

where  $u_c$  is velocity,  $s$  is channel slope, and  $C(Q)$  represents the very site-dependent relationship between velocity and channel shape and roughness that varies with discharge level,  $Q$ .

[22]  $C(Q)$  was estimated here by considering travel times late in the season, when almost all the meltwater originated from snowpacks at the head of the channel. By mid-June of 2002 and 2003, only the highest elevations were snow covered in the satellite images, and most of the streamflow originated from glaciers and snowfields surrounding Mount

Lyell, the highest peak in Yosemite National Park. During the second half of the melt season, peak timings at all small-basin gauges agreed to within less than one hour, so we assume that the hour of peak flow observed at Rafferty Creek is about the same as that at the head of Lyell Canyon. With this assumption, we measured the difference between the hours of peak flow at various gauges (Figure 3) and combined that with in-channel distances from the DEM (Figure 5) to estimate mean velocities for different channel sections at different discharge rates (Figure 6).

[23] Four sites along the Tuolumne River were used to estimate travel times and velocities: the headwater streams (represented by Rafferty Creek and the head of Lyell Canyon), the Lyell Fork gauge, the Glen Aulin gauge, and the Hetch Hetchy gauge (Figure 6a). For each of the three upstream sites, the difference in hour of peak flow between that site and Hetch Hetchy was used to estimate the in-channel travel time to Hetch Hetchy at different levels of discharge (Figure 6b). The dates shown coincide with periods when discharge levels and streamflow timing were stable for several days and when satellite images were available to verify that the snow line had retreated to near the headwaters of Lyell Canyon. Travel times were about twice as long on 29 June 2002, when  $10 \text{ m}^3 \text{ s}^{-1}$  of discharge were recorded at the nearby Happy Isles gauge (Figure 3), as on 14 June 2003, when  $40 \text{ m}^3 \text{ s}^{-1}$  of discharge were recorded (Figure 6). Thus the higher discharge rate coincided with the faster velocities.

[24] Average velocities were estimated for the three reaches between the four gauges (Figure 6c). By normalizing these velocities by the square root of the average slope for each reach, we estimated  $C(Q)$  at selected times and locations (Figure 6d). Along each reach,  $C(Q)$  increased with discharge.  $C(Q)$  also increased downstream as contributing areas and discharge rates increased. The highest calculated value was  $138 \text{ km h}^{-1}$ , for the reach between Glen Aulin and Hetch Hetchy on 14 June 2002. This value is much higher than the others, perhaps because of some errors in the snow cover analyses; e.g., perhaps, on that day, snowfields too small to appear on the satellite image were providing runoff from the northern drainage area, which is closer to the Hetch Hetchy gauge than Glen Aulin. Such an unaccounted for source would result in an earlier diurnal peak and erroneously high velocity estimates. On 14 June 2003, snow was visible in satellite images of the northern drainage area, so no velocity estimate was made for the reach below Glen Aulin. The lowest calculated value is  $16 \text{ km h}^{-1}$  for the reach between the headwater streams and the Lyell Fork gauge on 29 June 2002, which was the location and date of the lowest discharge levels. The mean value of  $C(Q)$  for all three reaches was  $64 \text{ km h}^{-1}$  on 14 June 2002 and  $28 \text{ km h}^{-1}$  on 29 June 2002. Combining these two mean values with slope measurements along the channel provides rough estimates of how travel times and velocities vary along the channel (Figures 6b and 6c, lines) at higher and lower discharge levels. The very high velocities downstream of Glen Aulin correspond to a canyon-like section of the Tuolumne River characterized by steep granite slopes, repeated waterfalls, and supercritical flow. Because the main roughness elements in this river section are large boulders, the velocity has the potential to increase dramatically between low flows and high flows, when the boulders

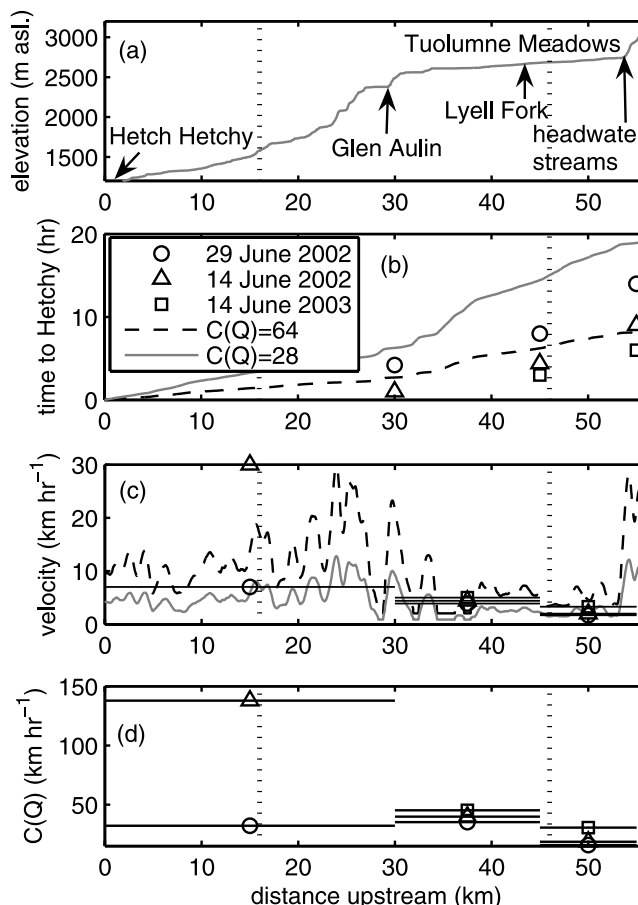


**Figure 6.** (a) Elevation versus distance along the main channel of the Tuolumne River, from Hetch Hetchy to the top of Mount Lyell. Vertical dashed lines indicate the location of the MODIS snow lines on 3 May and 3 June, near the start and peak of the 2003 melt season. (b) Travel time from a point along the channel to the Hetch Hetchy gauge as a function of distance. Travel times measured from hourly records of streamflow peaks are represented by circles (29 June 2002), triangles (14 June 2002), and squares (14 June 2003). The solid curve estimates travel time assuming  $v = 28\sqrt{s}$ , and the dashed curve estimates travel time assuming  $v = 64\sqrt{s}$ . (c) Estimated velocity versus distance along the same channel. Horizontal lines with symbols estimate average velocities for each reach between gauge measurements, for the same dates as in Figure 6b. Curves illustrate velocities from the same equations as in Figure 6b. (d)  $C(Q)$  for the same dates as in Figures 6b and 6c, calculated as  $C(Q) = \frac{\bar{v}}{\sqrt{s}}$  for each reach, where the bars denote average values.

become completely submerged [Bathurst, 2002]. From these velocity estimates and satellite maps of the snow line along the channel, travel times in the stream channel from the start to peak of the melt season can be approximated.

[25] Table 2 summarizes in-channel travel time estimates. For the Hetch Hetchy basin, the mainstream in-channel travel distance increased from 16 to 46 km, assuming that most melt originated from the edge of the snow line along the main channel. Estimated in-channel velocities increased from 7 to  $15 \text{ km h}^{-1}$ , assuming that the average values of

**Table 2.** Effects of Changing Snow Line and Water Velocity on Channel Travel Times in 2003

	$\langle x \rangle_{\text{initial}}$ 9 May, km	$\langle x \rangle_{\text{final}}$ 2 June, km	$u_{\text{initial}}$ km h <sup>-1</sup>	$u_{\text{final}}$ km h <sup>-1</sup>	$t_{\text{initial}}$ hours	$t_{\text{final}}$ hours	$\Delta t$ hours
Rafferty Creek	0	2	6	8	0	0.25	+0.25
Lyell Fork	0	9	1.7	3.3	0	2.7	+2.7
Hetch Hetchy	16	46	7	15	2.3	3.1	+0.8

$C(Q)$  of 28 and 64 km h<sup>-1</sup> are representative for low- and high-flow volumes, respectively. Channel length increased as the season progressed, as did flow velocity. The increased length (alone) would increase travel time; increased velocity would decrease travel time. The net effect of these two changes, however, was an increase in travel time by about +0.8 hours. If snow covered areas above the snow line contributed significantly to diurnal timing, the seasonal change in average travel distance in the channel would be smaller, and the increase in travel time would be smaller. If the velocity change was larger, which is possible since the range of discharge magnitudes between the starting and peak discharge values was greater than the range represented in the velocity estimates, the change in timing would be smaller and could become negative. Given these uncertainties (which would tend to reduce in-channel travel times), we will use the initial, longer travel time estimate in the following discussion.

[26] In contrast with the reach above Hetch Hetchy, travel times along the reach above the Lyell Fork gauge varied considerably with the retreating snow line (Table 2). Tuolumne Meadows is the flattest segment with the slowest flow velocities in the Tuolumne River basin (Figures 6a and 6c). Estimated in-channel velocities above the Lyell Fork gauge are about 10 times smaller than velocities above the Hetch Hetchy gauge (Figure 6c). These slow velocities result in large seasonal changes in channel travel time for meltwater originating upstream of Tuolumne Meadows (Figure 6b). At the start of the 2003 melt season, the entire Lyell Fork basin was covered with snow, so, assuming that most melt originated right next to the gauge, the channel section produced no delays. By the peak of the melt season, the snow line had moved 9 km upstream, so meltwater had to travel through 9 km of relatively flat meadows at perhaps 3 km h<sup>-1</sup> (Figure 6c). This increased the in-channel travel time by about 3 hours, a greater increase than that estimated for the larger Hetch Hetchy basin.

[27] Finally, above Tuolumne Meadows, in the steeper slopes of the headwater streams, in-channel velocities increased again (Figure 6), and travel distances in these small basins are short. Rafferty Creek was completely snow covered at the start of the 2003 melt season, and the snow line retreated 2 km by the season's peak. Estimated velocities for this reach varied from 6 to 8 km h<sup>-1</sup>, and the estimated seasonal increase in channel travel time is only about 15 min. Thus the time delay provided by increased travel distance was not enough to offset the 6-hour decrease in travel time observed in the snowpack in any of the Tuolumne River subbasins.

#### 2.4. Combined Travel Times

[28] Table 3 compares the estimated (from sections 2.1 and 2.3) and observed (from section 1) 2003 changes in hour of peak flow in the three subbasins. In Rafferty Creek a

headwater basin draining 25 km<sup>2</sup>, the stream channel is short, and the in-channel travel time has very little effect on the estimate of total travel time; thus we estimate that the 6-hour decrease in travel time through the snowpack should have been recorded at the stream gauge, as it was. In the intermediate-sized Lyell Fork basin (109 km<sup>2</sup>) the slow-velocity Lyell Canyon segment of the greater Tuolumne Meadows channel section, immediately upstream of the Lyell Fork gauge, introduced a delay of about 3 hours when the snow line retreated 9 km upstream of the gauge. Consequently, the estimated 6-hour decrease in travel time through the snowpack was partially offset by the estimated 3-hour increase in travel time in the channel, for a net decrease in travel time of about 3 hours, in agreement with observations that year. In the large Hetch Hetchy basin (775 km<sup>2</sup>), increasing channel velocities offset the delays due to increased travel distances in the estimated in-channel travel times (Table 2), so the maximum reasonable estimate of increased travel time was less than 1 hour. Combining this with the decreased time water spent in the snowpack yielded an estimated shift of daily peak flows to about 5 hours earlier at the peak of melt season than at the beginning. However, observations at Hetch Hetchy and other basins larger than 200 km<sup>2</sup> show that diurnal streamflow timing did not change during this period. Changing channel lengths alone are not enough to erase the influence of decreasing snow depth on diurnal cycle timing at the Hetch Hetchy basin scale.

### 3. Variable Velocity Model

[29] The order-of-magnitude arguments presented in Section 2 suggest that the channel geometry and changing snow line in the Hetch Hetchy basin do not explain the observed patterns in diurnal streamflow timing. This section applies the variable velocity model (VVM) developed by *Lundquist* [2004] and *Lundquist and Dettinger* [2005] to the Tuolumne River basin above Hetch Hetchy to determine whether, instead, heterogeneity of snowpack properties provides a better explanation for the scale dependence of the seasonal evolution of diurnal streamflow cycles. In one simulation, snow depths were only varied with elevation, so that snow uniformly ran out at lower elevations first, and the

**Table 3.** Estimated Versus Observed Changes in Time of Peak Flow for the First Month of Melt in 2003 for Three Tuolumne River Subbasins

2003	Change in Time of Peak Flow, hours	
	Estimated	Observed
Rafferty Creek	-6 + 0.25 = -5.75	-6
Lyell Fork	-6 + 2.7 = -3.3	-3
Hetch Hetchy	-6 + 0.8 = -5.2	0 (±1)

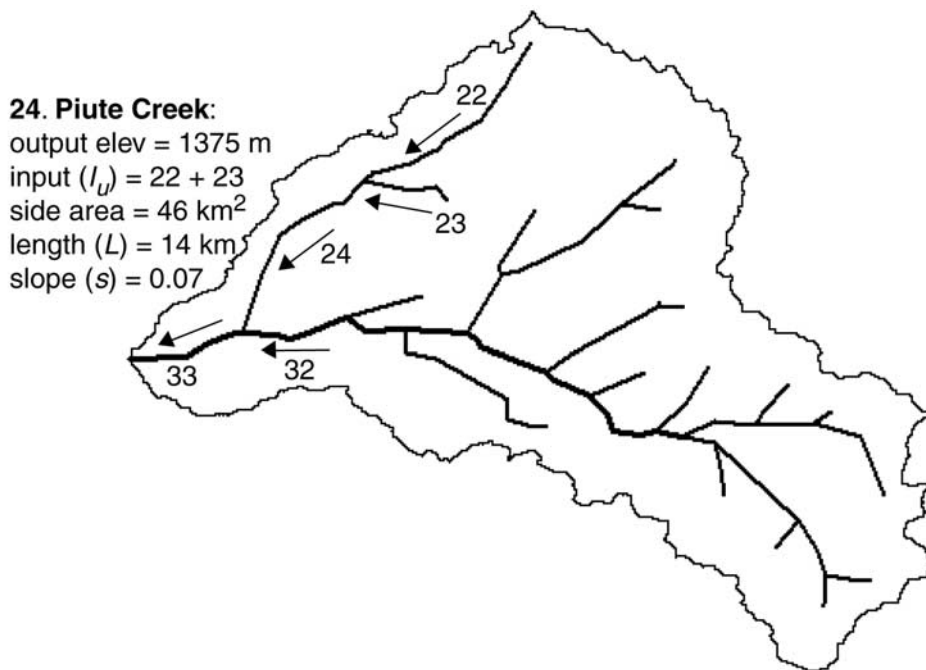


**Figure 7.** Map of Tuolumne River channels as represented in the VVM. Thick lines indicate channel segments. A new segment is defined each time a tributary stream intersects the main channel. The thin line delineates the boundaries of the Tuolumne River watershed above Hetch Hetchy. Numbers and arrows in the northwest corner of the diagram identify five channel segments. Each has unique properties measured from the DEM, as shown for segment 24, Piute Creek. The model considers 33 segments in total.

snow line retreated as observed in satellite images. In this simulation, snowpacks within each elevation band had identical properties. In a second simulation, snow depths were increased on average with elevation as in simulation 1. However, in this second simulation, snow depths and melt rates were also varied randomly within each elevation band. By comparing the diurnal cycles in the two simulations, the role of snowpack heterogeneity can be illustrated.

[30] The VVM represents the Tuolumne River as a series of channel segments (Figure 7), each with specified length, slope, contributing area, and mean elevation determined from the DEM. Segment lengths varied from 1 to 19 km, and slopes varied from 0.01 to 0.19. In both 2002 and 2003, SWE increased with elevation at the snow pillows. However, the relationship between melt rate and elevation was not significant at a 95% confidence level in either year, suggesting that elevation is not a dominant parameter controlling melt rates in this area. Spatially, melt rates vary much less than snow depth in alpine basins [Anderton *et al.*, 2002; Dunn and Colohan, 1999; Luce *et al.*, 1998; Hartman *et al.*, 1999]. Thus, for simplicity, we assumed that melt rates were not functions of elevation or location in the model. Initial snow depths were specified according to elevation (as outlined by Liston [1999]), so that, when the measured mean daily melt rates were integrated over the season, snow cover on average disappeared at each elevation on the first snow-free day observed by the MODIS satellite (Figure 8). A line fit to these SCA-based estimates, excluding the outlier at 0 cm initial SWE, indicates that average SWE increased 0.14 cm per m increase in elevation in 2003, with an initial average snow line at 2,400 m. This

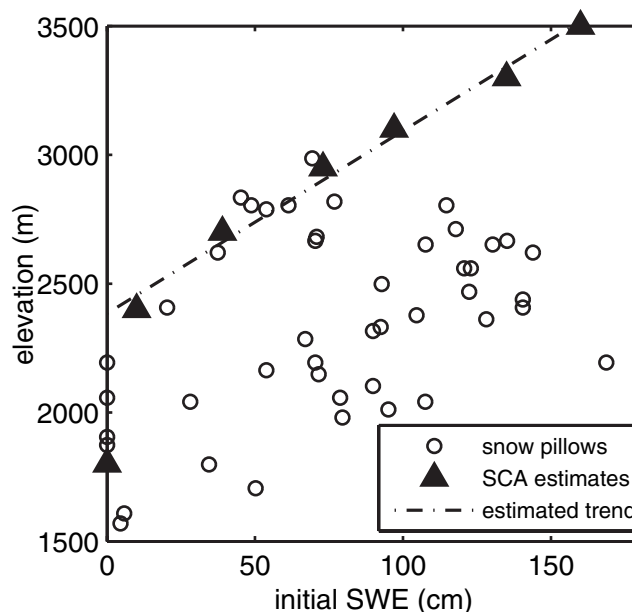


**Figure 8.** SWE as a function of elevation at the start of the 2003 melt season, measured from snow pillows (circles) and satellite images of changing snow-covered area (SCA, triangles). The dashed line represents the best linear fit to the SCA estimates, excluding the outlier with 0 cm initial SWE.

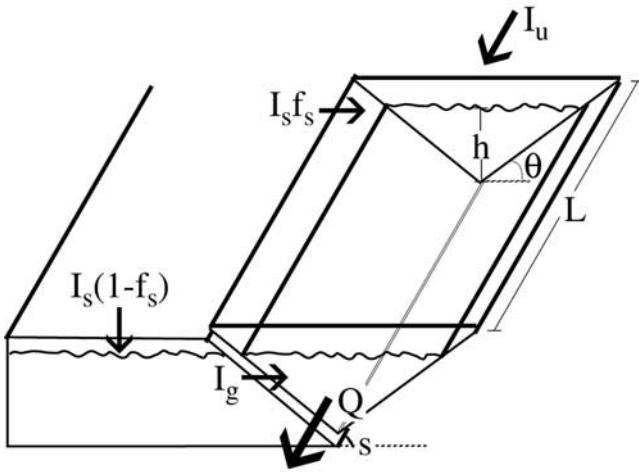


**Figure 9.** Diagram of river-routing component of the VVM.  $I_u$  is the upstream input,  $I_s$  is the local snowmelt input,  $f_s$  is the fraction of surface flow,  $I_g$  is the groundwater input,  $L$  is the length of the channel segment in this grid cell,  $h$  is the height of the water column,  $s$  is the slope of the channel bottom,  $\theta$  is the angle of the channel walls, and  $Q$  is the discharge from the channel segment (which will be  $I_u$  to the channel segment immediately downstream).

slope falls along the line of snow pillows with relatively low snow accumulation compared to other snow pillows at similar elevations (Figure 8). Because snow pillows are generally installed where large amounts of snow accumulate, they can overrepresent the snow depth for a given elevation. Also, because the MODIS snow-mapping algorithm [Hall *et al.*, 2000] only recognizes large patches of snow, the SCA may be set to zero before all the snow in a pixel is gone.

[31] The VVM models melted water's journey from the snowpack to the stream gauge in terms of two dominant stages. The first stage is the vertical propagation of meltwater through a snowpack, which introduces the asymmetry of the diurnal cycle [Lundquist and Cayan, 2002] and the shift in hour of peak flow to earlier in the day as the snow depth decreases. VVM disaggregates daily melt rates measured at snow pillows into half sinusoids with peaks at solar noon, and these hourly melts are input at the top of homogeneous or heterogeneous snowpacks. Water propagates independently through patches of snow with different initial depths and melt rates at a speed according to (2), following Dunne *et al.* [1976]. Faster melt pulses overtake slower ones, and shock fronts develop. Meltwater that reaches the bottom of all the snow patches along a given river segment at a given time is summed and input to the upper end of that adjoining channel segment.

[32] The second model stage is the flow of water down the channel to the gauge, with snowmelt at each channel segment adding to the flow from segments farther upstream as the water moves downstream (Figure 9). In the present simulations, the flux from the snowpack is first divided into 10% surface flow and 90% subsurface/groundwater flow, with fractions based on the observed relative amplitude of the diurnal cycle [Lundquist and Cayan, 2002]. The surface

flow is routed down the nearest channel using the Manning equation (following Henderson [1966] and Kouwen *et al.* [1993]), assuming  $V$ -shaped cross sections with constant side slopes,  $\theta$ , and spatially and temporally varying flow depths,  $h$ . From the Manning equation, the streamflow velocity,  $V$ , for this geometry is

$$V = \frac{1}{n} R^{2/3} \sqrt{s} = \frac{1}{n} \left( \frac{h \cos \theta}{2} \right)^{2/3} \sqrt{s} \quad (4)$$

where  $n$  is Manning's roughness coefficient,  $R$  is the hydraulic radius, and  $s$  is the longitudinal slope of the channel. The roughness coefficient,  $n$ , is assumed here to be 0.07, a value typical for mountain streams [Fread, 1993]. The side slope,  $\theta$ , is assumed to be  $18^\circ$ , based on channel cross sections measured from the DEM.  $C(Q)$  in equation (3) is represented more explicitly in equation (4) as a function of changing stream depths. The subsurface flow is modeled as outflow from a linear reservoir, which drains into the channel. Groundwater inflow,

$$I_g = K_g^{-1} S_g, \quad (5)$$

where  $K_g = 2.5$  days based on recession slopes from the Merced and Tuolumne Rivers, and  $S_g$  is the groundwater storage. Further model details and error analyses are presented by Lundquist [2004] and Lundquist and Dettinger [2005].

[33] In simulation 1, snowpack properties were kept uniform along each channel segment, with melt rates specified to equal the mean value measured by all the snow pillows each day and with the initial snow depths as shown in Figure 8 for that segment's mean elevation. In simulation 2, 100 independent snowpack patches were modeled alongside each channel segment. Each patch was prescribed a melt rate and depth chosen from a normal distribution with standard deviations as measured at the snow pillows and segment means as specified in simulation 1. For 2003, these standard deviations were 1 m for snow depths and  $1.5 \text{ cm d}^{-1}$  for melt rates. The areas of the 100 contributing patches were scaled by the segment's local contributing area, as measured in the DEM.

#### 4. Simulation Results

[34] Comparisons of observed discharge and hours of peak diurnal flows with simulated values for Rafferty Creek, Budd Creek, and Hetch Hetchy, are presented for spring 2003 (Figure 10) and spring 2002 (Figure 11). Rafferty and Budd creeks drain neighboring small basins of similar size and orientation (Figure 2), and streamflow peaks at nearly the same time each day in the two basins. Both records are shown in Figure 10 because the Rafferty Creek pressure sensor moved during seasonal peak flows in 2003, and there is some uncertainty about the measurements during the period from 28 May to 7 June 2003. At both Budd and Rafferty Creeks, continuous records of stream depth were converted to discharge magnitudes using rating curves established from at least 10 wading discharge measurements [Rantz, 1982] at each site. Since no discharge measurements were available at Hetch Hetchy, discharge was estimated as a linear multiple of depth. This yielded a

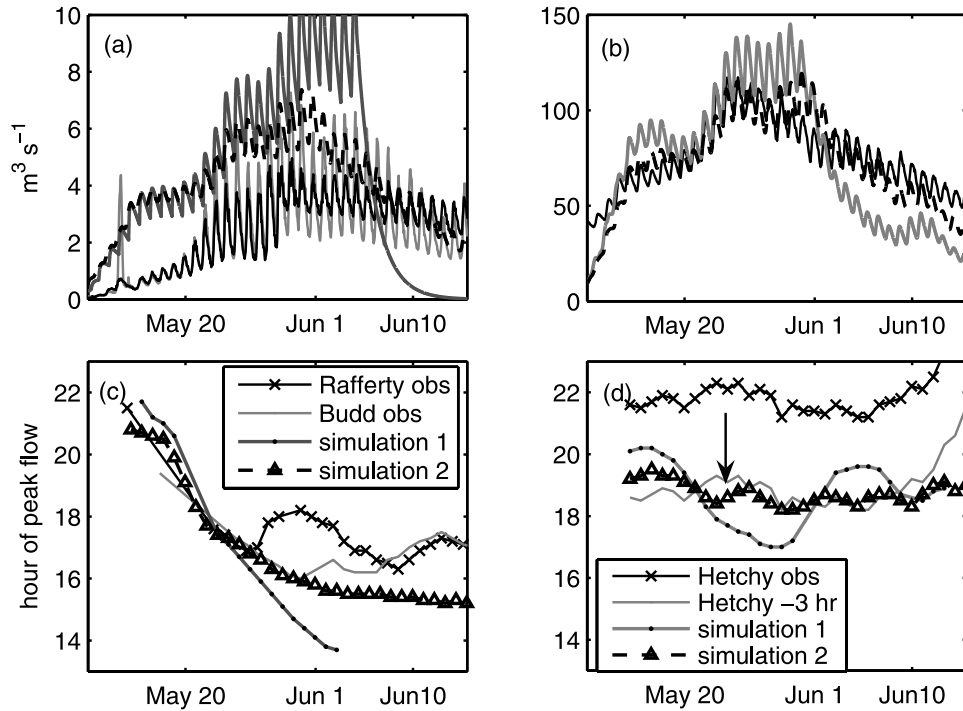


**Figure 10.** (a) Measured and simulated discharge versus time for two small basins, Rafferty and Budd creeks, for spring 2003. Observations are compared with simulations of Rafferty Creek, as marked in the legend in Figure 10c. (b) Estimated and simulated discharge versus time for the large basin, Hetch Hetchy, for 2003, with curves corresponding to the legend in Figure 10d. (c) Measured and simulated hour of peak streamflow versus time for the Rafferty and Budd Creek basins, for times corresponding to discharge levels in Figure 10a. (d) As in Figure 10c, but for the Hetch Hetchy basin. Observed flow timing at Hetch Hetchy is also plotted with an offset to 3 hours earlier, marked with arrow, for ease in comparison.

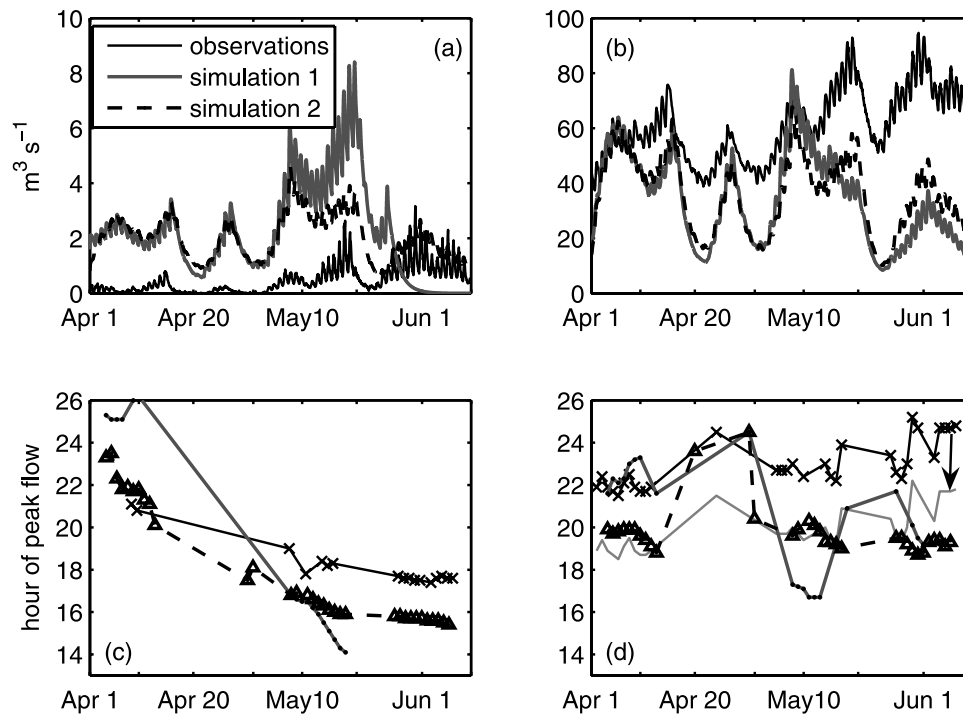


**Figure 11.** Same as Figure 10, except for 2002 and with no Budd Creek observations. Days where the time of peak of the diurnal cycle could be determined are marked with symbols in Figures 11c and 11d.

reasonable measure of the seasonal shape of the hydrograph but could not be used to check how accurately the model simulates discharge magnitudes.

[35] In the small basins (Figures 10a and 11a), both simulations 1 and 2 overestimated discharge magnitudes early in the season. This overestimate occurred because the entire basin was modeled as contributing melt during this period, whereas high-altitude stage measurements from the inflow to Fletcher Lake near Vogelsang (Figure 2) indicated that snow in some north facing basins above 3000 m began melting about 10 days later than at lower elevations. VVM specified melt rates independently of elevation because a better functional relationship could not be determined from the snow pillow measurements.

[36] Simulation 1 overestimated the small-basin seasonal peak discharges and dried out unrealistically during the late season (after 4 June 2003 and 25 May 2002). In this simulation, given the specified uniform character of each channel segment's snowpack, the entire segment area contributed melt until the mean snowpack was depleted. At that point, no refuge of snow remained to sustain late season flows. In contrast, the real world and simulation 2 both include snow covered areas long after the mean snowpack was gone.

[37] Simulation 2 incorporated heterogeneous snow properties, and, as a result, variable snow covered area along each segment. In this simulation, the basin's snowmelt contributions decreased more gradually. The longer-lasting snowpacks of simulation 2 generated late season discharges that agreed much better with observations. The improved agreement occurred because the thinnest snowpacks disappeared before peak melt. Peak discharge was lower because the thicker snowpacks covered only a fraction of the total basin area, producing less total meltwater. These thicker snowpacks also lasted longer into the season, producing larger late season discharges. Simulation 2 also appears to match the observed seasonal flows at Hetch Hetchy slightly better than did simulation 1 (Figures 10b and 11b). As in the smaller basins, simulation 1 overestimated early and peak seasonal discharge and underestimated late season discharge.

[38] In 2002, both simulations deviated more from observed flows than in 2003. This may be due to sustained stormy periods during spring 2002, which interfered with the normal progress of snowmelt. In VVM, storms were represented (crudely) by periods of "negative melt" which added SWE and depth to the snowpack but did not supply water to the streams. In the small high-elevation basins, e.g., Rafferty Creek, observations suggest these storms decreased the percentage of the basin with snow ripe for melting, which may have contributed to the simulations' large overestimation of discharge. At Hetch Hetchy, observations suggest that some water is added to the streams during these periods, perhaps from precipitation falling as rain at lower elevations. This may have contributed to the simulations' underestimation of discharge at Hetch Hetchy.

[39] In simulation 1, channel lengths increased as the snow line retreated, but there was no heterogeneity in snowpack properties along an individual channel segment. In this simulation, the times of peak daily flows shifted to earlier in the day during the early melt season in both small and large basins. In 2003, daily peak flows at Rafferty

Creek in simulation 1 arrived about 8 hours earlier by 30 May (day 150, the seasonal peak) than they did at the start of the melt season (Figure 10c). This shift is larger than the observed shift of 6 hours. In 2002, peak flow times in simulation 1 shifted to about 12 hours earlier between 1 April and 20 May, compared to an observed shift of about 4 hours (Figure 11c). In simulation 2, times of daily peak flows at Rafferty Creek in 2003 shifted about 6 hours earlier, in accord with observations. In 2002, simulated times of peak flows shifted 7.5 hours earlier, which is closer to observations than the results of simulation 1.

[40] At Hetch Hetchy, in both simulation 2 and in observations, daily peak flow times remained nearly constant in both years. However, in both 2002 and 2003, observed times of daily peak flow at Hetch Hetchy remained relatively constant near 2200 local time (Figures 10d and 11d), whereas the simulated times of peak flows at Hetch Hetchy were consistently about 1900 local time, 3 hours earlier. This offset may be due to an underestimate of channel roughness, resulting in overestimates of channel velocities. No wading discharge measurements were available to check velocities downstream of Glen Aulin. The too early simulations also may be due to delays introduced by hillslope travel times, which were not included in the model.

[41] In 2003, the time of peak flows in simulation 1 shifted to about 3 hours earlier in the early melt season, compared to the earlier estimate of 5 hours (section 2) and an observation of 0 hours (section 1). The shift of daily peak flows to earlier in the day in simulation 1 was interrupted at Hetch Hetchy after the season's peak discharge (30 May). By this time, the snow covered area had decreased to the point where most of the discharge originated upstream from Tuolumne Meadows, where slopes and velocities are relatively small. As more and more of the discharge at Hetch Hetchy originated above this break in channel slopes and in-channel velocities, the discharge-averaged travel times increased markedly. Simulation 2 matched observed changes in travel times well (Figure 10d). In 2002, Hetch Hetchy streamflow in simulation 1 peaked near 2200 at the beginning of the melt season and then shifted about 6 hours earlier near 10 May (Figure 11d). Flows in simulation 2 peaked near 1900 local time throughout most of the simulation (Figure 11d), with added delays of about 5 hours during the weeks with snowstorms in mid-April.

## 5. Summary, Discussion, and Applications

[42] Prior studies of nested basins [Braun and Slaymaker, 1981; Kobayashi and Motoyama, 1985] have suggested that the diurnal cycle in streamflow might yield information about snow characteristics in basins of all scales. This study examines nested basins across a wider range of areas and elevations, and demonstrates that diurnal streamflow timing is dominated by different characteristics at different basin scales. In small basins with limited elevation ranges and thus limited spatial variations in snow depths and melt rates, travel times through the snowpack dominate diurnal streamflow timing. Thus diurnal cycles reflect snow depths in these basins. In basins with areas less than 30 km<sup>2</sup>, the hour of daily peak flow generally occurs near midnight at the beginning of the season and then shifts to progressively earlier in the day.

[43] In larger basins that span large ranges of elevations and aspects, with greater spatial variations of snow depths, melt rates, and in-channel travel distances, snow heterogeneity and in-channel travel distances and velocities are more influential than the mean snow depth on the timing of diurnal cycles. Throughout the first half of the melt season, streamflow from these basins tends to peak consistently near midnight. As the melt season progresses, snow lines retreat to higher elevations, and higher elevations correlate with longer in-channel travel distances. However, during the first half of the melt season, increases in travel time due to increased distance are often offset by decreases in travel time due to increased velocity, as shown for the Hetch Hetchy basin in section 2. Thus both order-of-magnitude considerations and model simulations indicate that the retreat of the snow line is not sufficient to explain the near-constant time of peak flow observed at Hetch Hetchy from the start of the melt season until the day of peak discharge. Heterogeneity in snow depths and melt rates must be taken into account in order to properly simulate the near constancy of diurnal flow timings during this period. The same heterogeneity is necessary to reproduce the persistence of snowmelt-fed flows after the seasonal peak has passed. Thus snowpack heterogeneity is a fundamental part of the working of larger river basins.

[44] Pressure sensors for recording stream stage, such as those used in the Yosemite study, are small, inexpensive, easy to deploy, and have little environmental impact in remote mountain areas. Developing rating curves for sites in remote areas is labor intensive and time consuming, but precise information about diurnal cycle timing can be gleaned from stage information alone, without rating curves. Thus the ideas presented here provide practical ways to learn about snow and basin properties in remote, previously unmonitored basins. When all snowmelt input originates upstream, diurnal timing measured at different locations along a single channel gives direct measurements of travel time along channel segments. This information can be combined with distance and standard flow equations to estimate changing velocities and roughness coefficients for these segments at various levels of discharge (Figure 6).

[45] Diurnal timing in small basins, with areas less than 30 km<sup>2</sup>, provides information about snow water reserves throughout the melt season and might be used to forecast water supplies. Timing in larger river basins reflects the extent of heterogeneity within the basins. This may eventually provide an indicator of how many small basins should be monitored to adequately represent average snow depths contributing to the larger river's discharge. Timing in larger rivers is also remarkably consistent during the first half of the melt season each year, and this information can be used by hydroelectric power plants to predict the best hours of operation.

[46] Mountain channel morphology is characterized by pronounced and abrupt variations in slope [Wohl, 2000], and almost all mountain basins in the western United States have sections of very flat topography (generally lakes and meadows). The largest transitions in (in-channel) travel times are associated with periods when snowmelt patterns change from having most snowmelt derived from below a major flat segment (e.g., Tuolumne Meadows) to a pattern with most snowmelt deriving from above the break in slope.

Where low-gradient sections are long enough, they can introduce the abrupt onset of pronounced delays in diurnal cycle timing. When these sections are located at elevations upstream of a gauge, abrupt changes in diurnal cycle timing, which are likely to be repeated each year, may be used to determine the proportions of melt from upstream and downstream of the low-gradient section. A full examination of this effect is the subject of further research by the authors.

[47] Hourly discharge/stage information is already available in real time from 83% of USGS gauges (<http://waterdata.usgs.gov/nwis/rt>). In light of the results presented here, this data can be used to evaluate snowpack properties, basin heterogeneity, the location of snowmelt, or stream channel velocities in many settings. However, development of these methods will require the development of historical archives of hourly flows, which are not available for many gauges at present.

[48] **Acknowledgments.** The authors thank Jeff Dozier, Brad Werner, Rob Pinkel, and two anonymous reviewers for comments and suggestions on the manuscript. Brian Huggett and Jim Roche provided field support for the 2002 and 2003 Yosemite observations. Dave Peterson and Rich Smith provided the instruments and data for the Tuolumne River gauges at Hetch Hetchy and Highway 120, and Frank Gehrke and the California Snow Surveys provided snow sensor and snow survey data. Mammoth Mountain energy balance data were provided by Michael Colee and the NASA investigation "Hydrology, Hydrochemical Modeling, and Remote Sensing in Seasonally Snow covered Alpine Drainage Basins," the Donald Bren School of Environmental Science and Management at the University of California, Santa Barbara, the U.S. Army Corps of Engineers Cold Regions Research and Engineering Laboratory (CRREL), and the Mammoth Mountain Ski Area. Funding was provided by the Canon National Parks Foundation, the California Institute for Telecommunications and Information Technology, the U.S. Geological Survey, the NOAA Office of Global Programs through the California Application Program, the NSF ROADNet, and the California Energy Commission.

## References

- Adams, W. P. (1976), Areal differentiation of snow cover in east central Ontario, *Water Resour. Res.*, *12*, 1226–1234.
- Anderton, S. P., S. M. White, and B. Alvera (2002), Micro-scale spatial variability and the timing of snow melt runoff in a high mountain catchment, *J. Hydrol.*, *268*, 158–176.
- Bathurst, J. C. (2002), At-a-site variation and minimum flow resistance for mountain rivers, *J. Hydrol.*, *269*, 11–26.
- Bengtsson, L. (1981), Snowmelt generated run-off from small areas as a daily transient process, *Geophysica*, *17*, 109–121.
- Bras, R. L. (1990), *Hydrology: An Introduction to Hydrologic Science*, 643 pp., Addison-Wesley, Boston, Mass.
- Braun, L. N., and H. O. Slaymaker (1981), Effect of scale on complexity of snowmelt systems, *Nord. Hydrol.*, *12*, 235–246.
- Caine, N. (1992), Modulation of the diurnal streamflow response by the seasonal snowcover of an alpine basin, *J. Hydrol.*, *137*, 245–260.
- Colbeck, S. C. (1972), A theory of water percolation in snow, *J. Glaciol.*, *11*(63), 369–385.
- Colbeck, S. C., and E. A. Anderson (1982), The permeability of a melting snow cover, *Water Resour. Res.*, *18*(4), 904–908.
- Dettinger, M. D., and F. Gerkhe (2002), Thermodynamic evolution of snowpack at Gin Flat, Yosemite National Park, winter-spring 2002, paper presented at Sierra Nevada Science Symposium, U.S. Geol. Surv., Lake Tahoe, Calif.
- D'Odorico, P., and R. Rigon (2003), Hillslope and channel contributions to the hydrologic response, *Water Resour. Res.*, *39*(5), 1113, doi:10.1029/2002WR001708.
- Dunn, S. M., and R. J. E. Colohan (1999), Developing the snow component of a distributed hydrological model, a step-wise approach based on multi-objective analysis, *J. Hydrol.*, *223*, 1–16.
- Dunne, T. (1978), Field studies of hillslope flow processes, in *Hillslope Hydrology*, edited by M. J. Kirkby, pp. 227–293, John Wiley, Hoboken, N. J.
- Dunne, T., A. G. Price, and S. C. Colbeck (1976), The generation of runoff from subarctic snowpacks, *Water Resour. Res.*, *12*, 677–685.

- Elder, K., J. Dozier, and J. Michaelsen (1991), Snow accumulation and distribution in an alpine watershed, *Water Resour. Res.*, 27, 1541–1552.
- Erxleben, J., K. Elder, and R. Davis (2002), Comparison of spatial interpolation methods for estimating snow distribution in the Colorado Rocky Mountains, *Hydrol. Processes*, 16, 3627–3649.
- Fread, D. L. (1993), Flow routing, in *Handbook of Hydrology*, edited by D. R. Maidment, pp. 10.1–10.36, McGraw-Hill, New York.
- Grover, N. C., and A. W. Harrington (1966), *Stream Flow: Measurements, Records and Their Uses*, 363 pp., Dover, Mineola, N. Y.
- Hall, D. K., G. A. Riggs, and V. V. Salomonson (2000), MODIS/Terra Snow Cover 8-Day L3 Global 500m Grid V004, <http://arcss.colorado.edu/data/mod10a2.html>, Natl. Snow and Ice Data Cent., Boulder, Colo. (Updated weekly.)
- Hartman, M. D., J. S. Baron, R. B. Lammers, D. W. Cline, L. E. Band, G. E. Liston, and C. Tague (1999), Simulations of snow distribution and hydrology in a mountain basin, *Water Resour. Res.*, 35, 1587–1603.
- Henderson, F. M. (1966), *Open Channel Flow*, 522 pp., Macmillan, New York.
- Jordan, P. (1983), Meltwater movement in a deep snowpack: 1. Field observations, *Water Resour. Res.*, 19, 971–978.
- Kattelmann, R., and J. Dozier (1999), Observations of snowpack ripening in the Sierra Nevada, California, U.S.A., *J. Glaciol.*, 45(151), 409–416.
- Kobayashi, D., and H. Motoyama (1985), Effect of snow cover on time lag of runoff from a watershed, *Ann. Glaciol.*, 6, 123–125.
- Kouwen, N., E. D. Soulis, A. Petroniro, J. Donald, and R. A. Harrington (1993), Grouping response units for distributed hydrologic modeling, *J. Water Resour. Plann. Manage.*, 119(3), 289–305.
- Liston, G. E. (1999), Interrelationships among snow distribution, snowmelt, and snow cover depletion, implications for atmospheric, hydrologic and ecologic modeling, *J. Appl. Meteorol.*, 38, 1474–1487.
- Logan, L. (1973), Basin-wide water equivalent estimation from snowpack depth measurements, in *Role of Snow and Ice in Hydrology, IAHS AIHS Publ.*, 107, 864–884.
- Luce, C. H., D. G. Tarboton, and K. R. Cooley (1998), The influence of the spatial distribution of snow on basin-averaged snowmelt, *Hydrol. Processes*, 12, 1671–1683.
- Lundquist, J. D. (2004), The pulse of the mountains: Diurnal cycles in western streamflow, Ph.D. thesis, Univ. of Calif., San Diego, La Jolla.
- Lundquist, J. D., and D. Cayan (2002), Seasonal and spatial patterns in diurnal cycles in streamflow in the western United States, *J. Hydrometeorol.*, 3, 591–603.
- Lundquist, J. D., and M. D. Dettinger (2005), How snowpack heterogeneity affects diurnal streamflow timing, *Water Resour. Res.*, 41, W05007, doi:10.1029/2004WR003649.
- Lundquist, J. D., D. R. Cayan, and M. D. Dettinger (2003), Meteorology and hydrology in Yosemite National Park: A sensor network application, in *Information Processing in Sensor Networks: Second International Workshop, IPSN 2003*, edited by F. Zhao and L. Guibas, pp. 518–528, Springer, New York.
- Lundquist, J. D., D. R. Cayan, and M. D. Dettinger (2004), Spring onset in the Sierra Nevada: When is snowmelt independent of elevation?, *J. Hydrometeorol.*, 5, 325–340.
- Rantz, S. E. (1982), *Measurement and Computation of Streamflow*, vol. 1, *Measurement of Stage and Discharge*, U.S. Geol. Surv. Water Supply Pap., 2175, 284 pp.
- Rickenmann, D. (1994), An alternative equation for the mean velocity in gravel-bed rivers and mountain torrents, in *Hydraulic Engineering '94: Proceedings of the 1994 Conference*, pp. 672–676, Am. Soc. of Civ. Eng., Reston, Va.
- Shook, K., and D. M. Gray (1997), Synthesizing shallow seasonal snow covers, *Water Resour. Res.*, 33, 419–426.
- Smith, J. L. (1974), Hydrology of warm snowpacks and their effects upon water delivery...some new concepts, in *Proceedings, Symposium on Advanced Concepts and Techniques in the Study of Snow and Ice Resources, Monterey, CA., Dec. 2–6, 1973*, pp. 76–89, Natl. Acad. of Sci., Washington, D. C.
- Wohl, E. (2000), *Mountain Rivers*, *Water Resour. Monogr.*, vol. 14, 320 pp., AGU, Washington, D. C.
- Woo, M., and H. O. Slaymaker (1975), Alpine streamflow response to variable snowpack thickness and extent, *Geogr. Ann.*, 57, 201–212.
- 
- D. R. Cayan, Scripps Institution of Oceanography, 9500 Gilman Drive, La Jolla, CA 92093, USA.
- M. D. Dettinger, U.S. Geological Survey, La Jolla, CA 92093, USA.
- J. D. Lundquist, CIRES, Climate Diagnostics Center, University of Colorado, 216 UCB, Boulder, CO 80309-0216, USA. (jessica.lundquist@noaa.gov)